Advanced Journal of Chemistry-Section A

Original Research Article

Fe₃O₄@SiO₂-NH₂/CoSB Modified Carbon Paste Electrode for Simultaneous Detection of Acetaminophen and Chlorpheniramine

Sajjad Azimi, Mandana Amiri* ⬤, Hamideh Imanzadeh, Abolfazl Bezaatpour

Deapartment of Chemistry, University of Mohaghegh Ardabili, Ardabil, Iran

ARTICLE INFO

ABSTRACT

In this work, a cobalt Schiff base complex (CoSB) immobilized at the surface of Fe₃O₄@SiO₂-NH₂ nanoparticles was synthesized and characterized using different characterization techniques such as Scanning electron microscopy (SEM), Fourier transform infrared (FT-IR) spectroscopy, X-ray diffraction (XRD). The prepared nanocomposite (Fe₃O₄@SiO₂-NH₂/CoSB) was applied as a sensitive modifier in carbon paste electrode (CPE) for simultaneous determination of acetaminophen (AC) and chlorpheniramine (CP). The Fe₃O₄@SiO₂-NH₂/CoSB/CPE exhibited good electrochemical response towards the detection of AC and CP. In addition, an excellent separation between the voltammetric signals for these analytes at the surface of modified electrode was observed. The suggested method was effectively employed for concentration variation studies of a mixture containing these drugs. The dynamic linear ranges of 5.0×10^{-7} to 1.0×10^{-3} M and 8.0×10^{-6} to 1.0×10^{-3} M with detection limits 4.0×10^{-7} M and 5.0×10^{-6} M (for S/N = 3) were achieved for AC and CP, respectively. The performance of the presented electrochemical nanosensor was assessed by quantifying the two drugs in spiked human blood serum and in tablets.

GRAPHICAL ABSTRACT
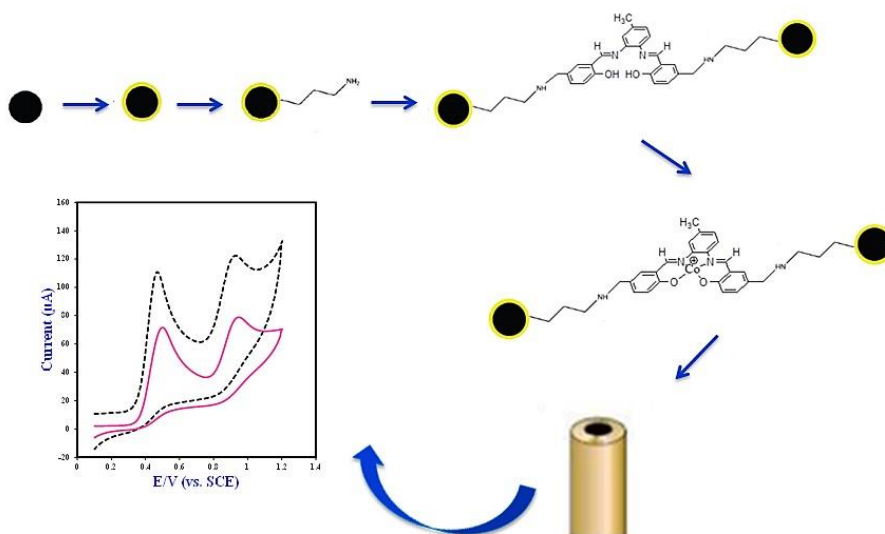
* Corresponding author: Amiri, Mandana

✉ E-mail: mandanaamiri@uma.ac.ir

Introduction

Acetaminophen (AC, N-acetyl-p-aminophenol), more popularly known as paracetamol, is commonly utilized to suppress pain and fever [1]. AC is also employed to treat postoperative analgesia, migraine pain, neurodynia and arthralgia [2,3]. Moreover, owing to similar working mechanism to aspirin, AC can replace aspirin for patients with allergies [4]. However overuse of this drug causes the accumulation of toxic metabolites that can damage the kidneys and liver [5]. Chlorpheniramine (CP, [3-(4-chlorophenyl)-3-(pyridin-2-yl) propyl]dimethyl-amine) is a strong first-generation alkyl amine antihistamine usually used to relieve allergic diseases and common cold [6,7]. Allergic symptoms include itchy or watery eyes, cough, sneezing, runny nose, urticaria and rash. CP is also effective against motion sickness and nausea [8]. Given the extensive use of AC and CP all over the world, it is important to determine their level of traceability since the regimen of these drugs has a high importance in biological samples and has an immense influence on health. Therefore, a sensitive, appropriate and accurate analytical technique should be developed for the simultaneous detection of AC and CP.

So far, numerous analytical techniques have been developed to attain the sensitive detection of AC and CP, such as high-performance liquid chromatography [9-12], spectrophotometry [13, 14] and mass spectrometry [15, 16]. Although most proposed methods have been successfully employed, they still face major challenges such as the much material consumption, expensive reagents and instruments, time-consuming and complicated sample pretreatments.

Compared with the above techniques, electrochemical methods using modified electrodes offer a rapid, inexpensive, accurate, real-time analytical path through simple operations with high selectivity and sensitivity [17, 18]. The high-performance electrochemical sensing of detecting target molecules is significantly dependent on the electrode materials, so the select of electrode material is highly crucial.

In recent years, nano-materials have been found a broad application in the design and development of modified electrodes in electrochemical sensors. Among the different nano-materials, magnetic Fe_3O_4 nanoparticles (Fe_3O_4 NPs) have attracted a considerable attention due to their high surface area-to-volume ratio, superb magnetic properties, great surface energy, low toxicity and easy preparation [19]. However, these nanoparticles are not stable in air due to their high surface energy and easily aggregation. Also, the lack of active group limits their further usage in electrochemical sensors. In order to overcome the above problems, Fe_3O_4 NPs are protected with a shell of silica that can not only avoid Fe_3O_4 NP aggregation but also be functionalized simply to increase adaptability [20].

In addition, Schiff base complexes are an attractive class of compounds that have found a broad range of applications in various fields due to their intriguing physical and chemical properties. They can be easily coordinate with most of the transition metals and create stable metal Schiff base complexes. Metal Schiff-base complexes are often used as catalysts for the electrochemical determination of pharmaceutical and biological compounds under various conditions [21-23].

In this research study, we successfully synthesized of a novel nanocomposite based on amine-functionalized silica coated magnetic nanoparticles and cobalt Schiff base complex ($Fe_3O_4@SiO_2$-NH_2/CoSB). The synthesized nanocomposite was identified by XRD, FT-IR, and SEM. $Fe_3O_4@SiO_2$-NH_2/CoSB was used as a sensitive modifier in carbon paste electrode to fabricate a new electrochemical nanosensor for simultaneous measurement of AC and CP. The proposed nanosensor showed an outstanding

performance for simultaneous measurement of AC and CP. Also, the applicability of the suggested electrochemical detection system for both compounds based on CPE/Fe$_3$O$_4$@SiO$_2$-NH$_2$/CoSB was examined using real samples.

Experimental

Reagents and materials

Acetaminophen (AC) and chlorpheniramine (CP) were kindly donated by Zahravi Pharmaceutical Co., Iran. The other chemicals are: Potassium acetate (CH$_3$CO$_2$K, Rankem, India), monopotassium phosphate (KH$_2$PO$_4$, Rankem, India), acetic acid (CH$_3$CO$_2$H, Merck, Germany), citric acid (C$_6$H$_8$O$_7$, Rankem, India), phosphoric acid (H$_3$PO$_4$, Merck, Germany), potassium chloride (KCl, Rankem, India), potassium hydroxide (KOH, Rankem, India), ammonia (NH$_3$, Rankem, India), iron (III) chloride hexahydrate (FeCl$_2$.4H$_2$O, Rankem, India), iron (II) chloride tetrahydrate (FeCl$_3$.6H$_2$O, Rankem, India), dichloromethane (DCM, CH$_2$Cl$_2$, Royalex), cobalt(II)acetate tetrahydrate (Co(CH$_3$COO$^-$)$_2$.4H$_2$O, Merck, Germany), tetraethyl orthosilicate (SiC$_8$H$_{20}$O$_4$, Merck, Germany), sodium perchlorate (NaClO$_4$, Merck, Germany), (3-Aminopropyl) triethoxysilane (C$_9$H$_{23}$NO$_3$Si, Aldrich, chine). All required solutions were prepared with deionized (DI) water (>18 MΩ cm). In addition, human serum was prepared from Iranian Blood Transfusion Organization (IBTO) and stored at -20°C. The buffers employed were phosphate buffer (PB, 0.1 M) for pH 2.0, 3.0, 6.0, 7.0 and acetate buffer (AB, 0.1M) for pH 4, 5.Stock solutions of AC and CP were prepared by dissolving a proper amount of drugs in DI water.

Apparatus and electrochemical measurements

All electrochemical experiments were done on a Voltammetric Analyzer (Metrohm Computrace, model 797 VA, Switzerland). A standard three

electrode system was employed by a carbon paste electrode (CPE, 3 mm diameter) as the working electrode, saturated Calomel as the reference electrode (SCE; Hg/Hg$_2$Cl$_2$/Cl$^-$) and a platinum wire as the counter electrode. The morphologies of the materials were investigated with a scanning electron microscope ((SEM, LEO 1430 VP model, Germany). Fourier transform infrared (FT-IR) spectra were carried out using a Perkin-Elmer instrument. X-ray diffraction patterns were recorded on an X-ray diffract meter (Philips, Netherlands). The scanning angles were in the range of 2θ = 10–80° at room temperature.

Fe$_3$O$_4$@SiO$_2$-NH$_2$/CoSB synthesis

Fe$_3$O$_4$@SiO$_2$-NH$_2$/CoSB was synthesized in three steps.

Step I: Fe$_3$O$_4$@SiO$_2$-NH$_2$

First, Fe$_3$O$_4$ nanoparticles (Fe$_3$O$_4$NPs) were synthesized by chemical co-precipitation method according to the earlier report [24]. Then, SiO$_2$ shells were coated on the surface of the synthesized Fe$_3$O$_4$NPs according to the following procedure: 1 g of Fe$_3$O$_4$NPs was added to 31 mL of citric acid solution and its pH was then adjusted to 5.8 by ammonia. The above obtained solution was stirred (80-90°C, 90 min) under reflux conditions. Again after 90 min the pH of the solution with ammonia was set to 11. Then, 1.2 mL of tetraethoxysilane (TEOS) was added dropwise into the reaction vessel. After stirring for 24 h, the resulted suspension was collected by strong magnet and washed several times with distilled water and ethanol [25, 26]. Next, the Fe$_3$O$_4$@SiO$_2$ nanoparticles were functionalized by 3-ammonia propyl triethoxy silane (APS) [27]. Briefly, to functionalize the Fe$_3$O$_4$@SiO$_2$ nanoparticles, 3 mL of APS was dissolved mL 100 mL ethanol and added dropwise to the Fe$_3$O$_4$@SiO$_2$ solution with continuous stirring and its pH was then adjusted to 11 by KOH. The reaction continued for 5 h under stirring at 70°C.

After 5 h, the precipitate was separated by a strong magnet and washed repeatedly with distilled water.

Step II: $Fe_3O_4@SiO_2-NH_2$-Schiff base

5-chlormethylene Salophen was synthesized by addition of 5-chloromethyl-2-hydroxybenz-aldehyde (0.825 g in 5 mL DCM) to 4-Methyl-*o*-phenylenediamine (0.311 g in 5 mL DCM). After 4 hours of reflux, the resulting yellow precipitate was filtered and washed several times with DCM. Then, 10 mg synthesized Schiff bas was dispersed in 30 mL ethanol and added to 50 mL

of the $Fe_3O_4@SiO_2-NH_2$. Next, the reaction was continued under reflux and magnetic stirring for 24 h [22].

Step III: $Fe_3O_4@SiO_2-NH_2/CoSB$

In the last stage, 2.9 g of cobalt (II) acetate tetrahydrate, 2.1 g of sodium perchlorate and 1 mL of pyridine were added to the reaction vessel containing $Fe_3O_4@SiO_2-NH_2$/Schiff Base, and then aerated for 4 h. The resulting precipitate was collected by a strong magnet and washed with methanol.

Scheme 1. The fabrication steps of the $Fe_3O_4@SiO_2-NH_2/CoSB$.
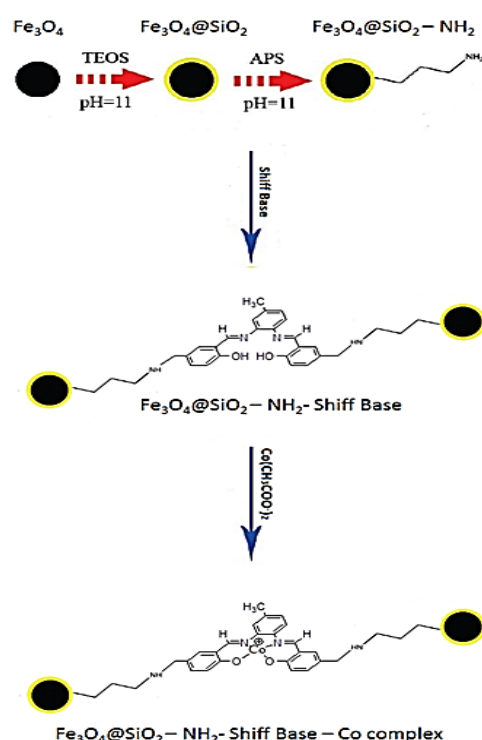
Modified electrode preparation

The CPE was fabricated by mixing graphite powder with paraffin oil in the ratio ~75:25 (w/w) in a mortar and eroded for 20 min. To form completely homogeneous paste, a few milliliters of DCM was added to it and stirred thoroughly. The resulting homogeneous mixture remained at room temperature for several hours till the DCM is completely evaporated. Then, a portion of the obtained mixture was filled into the end of a Teflon tube (3 mm i.d.). A copper

wire was attached to the other end of the tube to create electrical contact. For the preparation of modified CPE, when making carbon paste with graphite and paraffin, as-synthesized nanocomposites, (5% w) was added to the carbon paste.

Preparation of real samples

Commercial pharmaceutical tablets were examined to check the validity of the suggested nanosensor. To obtain each pharmaceutical

formulation, five tablets of each brand (AC and CP) were weighted and grinded with mortar and pestle, separately. Then, an accurately weighed portion of the powder dissolved in the desired buffer. The contents were sonicated for 15 min to separate impurities from the tablet. Finally, using filter paper, the resulting solution was filtered and the sub-filter solution was used for the electrochemical measurements.

Analytical utility of the proposed method was also investigated using human serum sample. First, blood serum sample was transferred to centrifuge tubes, and then 2 mL of methanol was added for every 5 mL of serum. Methanol was applied as a precipitating agent to remove blood serum proteins. After centrifugation, clear supernatant layers were filtered and collected. The standard addition technique was utilized for the quantification of AC, and CP and calculation of recovery values in the real samples.

Results and Discussion

Characterization of Fe$_3$O$_4$@SiO$_2$-NH$_2$/CoSB

In order to gain the crystallographic information about the Fe$_3$O$_4$ nanoparticles and silica-coated Fe$_3$O$_4$ nanoparticles, X-ray diffraction (XRD) analysis was applied. Figure 1A illustrates the XRD pattern of the Fe$_3$O$_4$NPs. As can be observed, in the XRD pattern of the Fe$_3$O$_4$ nanoparticles, eight main peaks located at 2θ values of 30.5°, 35.8°, 43.4°, 53.8°, 57.4°, 62.9° and 74.5° correspond to the following Fe$_3$O$_4$NPs cubic spinel planes: (220), (311), (400), (422), (511), (440), and (533), respectively. This pattern is fully consistent with the standard XRD pattern for magnetite provided by JCPDS (no. 19-0629). It can also be seen from Fig 1A that after modification magnetite nanoparticles with silica, crystal structure of Fe$_3$O$_4$ remains unchanged. In addition the diffraction peak at 2θ value of 20 ° confirms the presence of silica [26, 28].

The Scherer's formula was applied to calculate the average crystallite sizes of the magnetic nanoparticles from the peak appears at about 35.82° (plane 311) according to the equation(1):

$$D = k\lambda / \beta\cos\theta \qquad (1)$$

In this equation, "D" is the crystalline size (in nm), "K" is a dimensionless constant near to 0.99, "λ" is the wavelength of the employed X-ray (in nm), "β" is the full width at half maximum (FWHM, in radian) and "θ" is the Bragg angle in radians. The average size of Fe$_3$O$_4$ nanoparticles was calculated 38 nm.

Scanning electron microscopy (SEM) was applied to evaluate the morphological characteristics of Fe$_3$O$_4$NPs and Fe$_3$O$_4$@SiO$_2$-NH$_2$/CoSB. The obtained images of Fe$_3$O$_4$NPs (B) and Fe$_3$O$_4$@SiO$_2$-NH$_2$/CoSB (C) are displayed in Figure 1. As can be seen in Figure 1B, most of Fe$_3$O$_4$ nanoparticles exhibit spherical structure with average particle sizes of about 35-45 nm, which is in consistent consent with estimated value by Scherrer equation (38 nm). Also, the magnetic nanoparticles modified with Schiff base complex reveal larger particle size of 50-56 nm that this increase in particle size is due to the coating of silica on the magnetic nanoparticles (Figure 1C) [26].

Comparative FT-IR spectra of Fe$_3$O$_4$ (curve a), 5-chlormethylene Salophen Schiff Base (curve b), Fe$_3$O$_4$@SiO$_2$-NH$_2$/Schiff Base (curve c) and Fe$_3$O$_4$@SiO$_2$-NH$_2$/CoSB (curve d) are depicted in Figure 2. The FT-IR spectrum of Fe$_3$O$_4$ exhibits two significant peaks at 590 and 3595 cm^{-1} corresponding to Fe–O and Fe–OH bands. The FT-IR spectrum of Schiff Base exhibits the absorption peak in the 1620 cm^{-1} region, which is ascribed to the stretching vibration of C=N. Also, the appearance of this peak in the curves c and d is evidence of the successful stabilization of the Schiff base on the surface of the magnetite nanoparticles [26].

The cyclic voltammetry technique was used to

Figure 1. XRD pattern of Fe_3O_4 NPs and $Fe_3O_4@SiO_2$ (A), SEM image of Fe_3O_4 NPs (B) and $Fe_3O_4@SiO_2$-NH_2/CoSB (C).
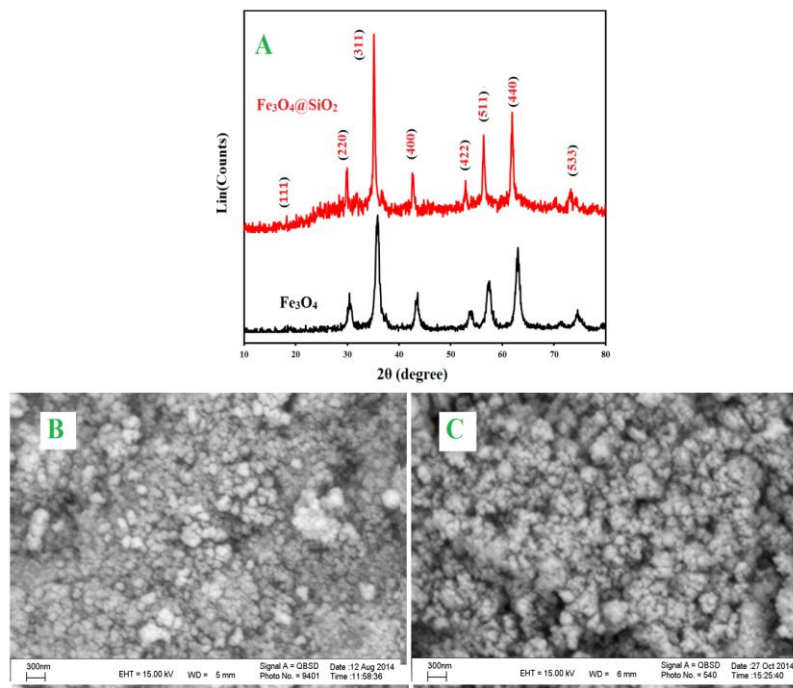
Figure 2. FT-IR spectra of Fe_3O_4, 5-chlormethylene Salophen Schiff Base, $Fe_3O_4@SiO_2$-NH_2/Schiff Base and $Fe_3O_4@SiO_2$-NH_2/CoSB.
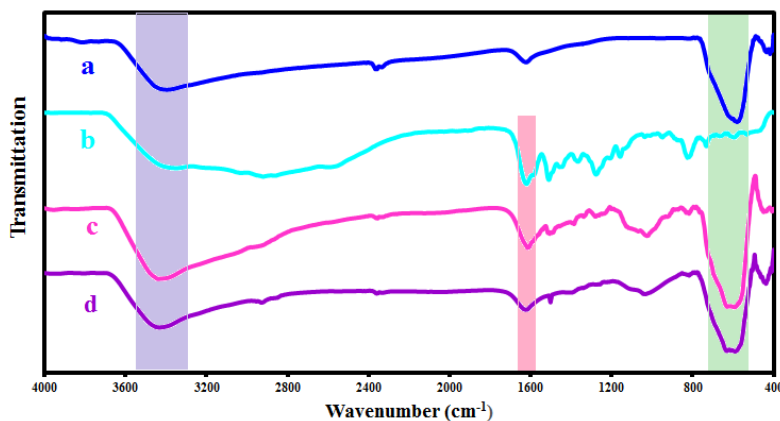
examine the electrochemical behavior of the unmodified and modified CPE. For this purpose, cyclic voltammograms of modified and unmodified electrode in 0.1 M phosphate buffer (pH 2, 7) within the potential range between -0.4 and 1.0 V were recorded and compared (data not shown). The CV responses indicated no peak at the surface of electrodes in the studied potential ranges. This indicates that there is no interference with the simultaneous measurement of these two drugs. In addition, the increase in capacitive current of the modified electrode compared to the bare electrode indicates an increase in active electrode surface area.

Electrochemical behavior of AC and CP on CPE/Fe$_3$O$_4$@SiO$_2$-NH$_2$/CoSB

The electrochemical behavior of the AP and CP molecules was studied by using the cyclic voltammetry technique at the bare and modified CP electrodes. Figure 3A and 3B illustrate the CVs recorded at the surface of bare CPE and CPE/Fe$_3$O$_4$@SiO$_2$-NH$_2$/CoSB in the presence of 1 mM AC (Figure 3A) in PB (0.1 M, pH 4.0) and CP

(Figure 3B) in PB (0.1 M, pH 7.0) with scan rate of 100 mV s^{-1}. As seen in Figure 3A, bare CPE displayed a broad oxidation peak with low peak current (67μA) for AC at 0.45 V, suggesting a weak and sluggish electron transfer rate at the surface of bare CPE. While a sharp anodic peak (113μA) for AC is obtained using CPE/Fe$_3$O$_4$@SiO$_2$-NH$_2$/CoSB. Similarly, the same behavior was observed for CP (Figure 3B). The increasing peak current for oxidation of CP was from 31 μA to 48.8 μA accompanied with peak

potential shift to less positive potentials at the surface of CPE/Fe$_3$O$_4$@SiO$_2$-NH$_2$/CoSB. A lower overpotential combined with a higher anodic peak current for the oxidation of AP and CP compounds on the CPE/Fe$_3$O$_4$@SiO$_2$-NH$_2$/CoSB illustrates that the rate of an electron transfer can be accelerated by anchoring of a Co-Schiff base complex onto silica-coated magnetic nanoparticles leading to a high electrocatalytic activity and an improved efficiency of the electrode.

Figure 3. CV curves of bare CPE and CPE/Fe$_3$O$_4$@SiO$_2$-NH$_2$/CoSB (dashed line) recorded for 1mM AC in PB (0.1M, 4.0) (A) and 1mM in PB (0.1M, 7.0) (B) at scan rate 100 mV s^{-1}.
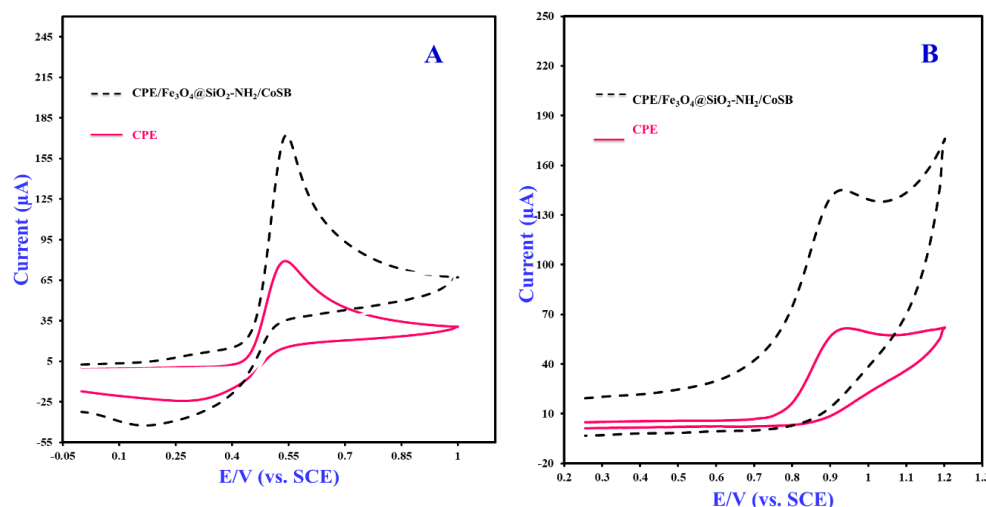
Effect of Scan Rate

Cyclic voltammograms of 1mM of AC (Figure 4A) and CP (Figure 4C) were acquired on the surface of the CPE/Fe$_3$O$_4$@SiO$_2$-NH$_2$/CoSB at different scan rates (10-200 mV.s^{-1}) to study the effect of sweep rate on the peak potential (E$_{pa}$) and peak current (I$_{pa}$). The results showed that for CP no reduction peak is observed on the reverse scan in different scan rates. This demonstrates a completely irreversible process for CP. However, the intensity of the cathodic peak for AC becomes notable at higher scan rates. Also, the anodic peak intensities were continuously increased upon increasing the scan rate, and the peak potential was slightly shifted to higher side for both analytes. A linear relationship was achieved between the peak

height and the square-root of scan rate ($υ^{1/2}$) according to following equations:

I_{pa} (μA) for AC = 257.94 $υ^{1/2}$ + 2.554 (R^2 = 0.999)

I_{pa} (μA) for CP = 116.03 $υ^{1/2}$ – 3.869 (R^2 = 0.995)

This behavior confirms that the electrochemical processes of AC and CP on CPE/Fe$_3$O$_4$@SiO$_2$-NH$_2$/CoSB are diffusion-controlled processes.

Effect of pH on voltammetric peaks of AC and CP

The influence of sample solution pH on the oxidation peak potentials and currents of AC and CP on the surface of the CPE/Fe$_3$O$_4$@SiO$_2$-NH$_2$/CoSB was examined in the pH range of 2.0–8.0 employing acetate and phosphate buffer, as depicted in Figure 5A-C. The results exhibited

Figure 4. Effect of scan rate on CV curves of 1 mM of AC in PB (0.1M, 4.0) (A and B) and 1 mM of CP in PB (0.1M, 7.0) (C and D) observed at the surface of CPE/Fe$_3$O$_4$@SiO$_2$-NH$_2$/CoSB.
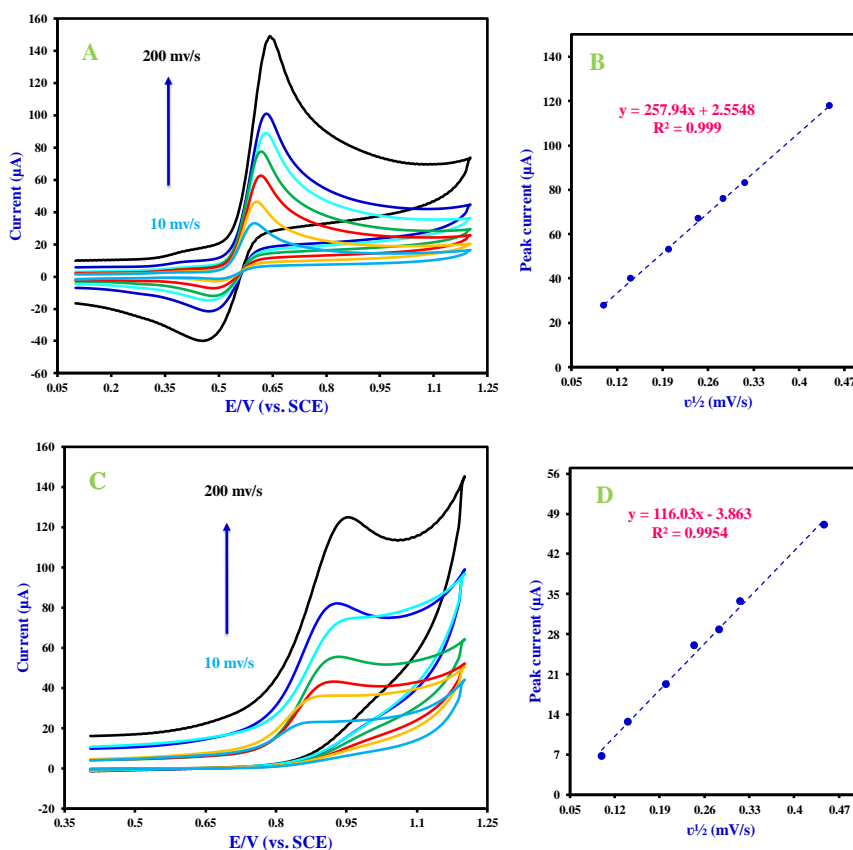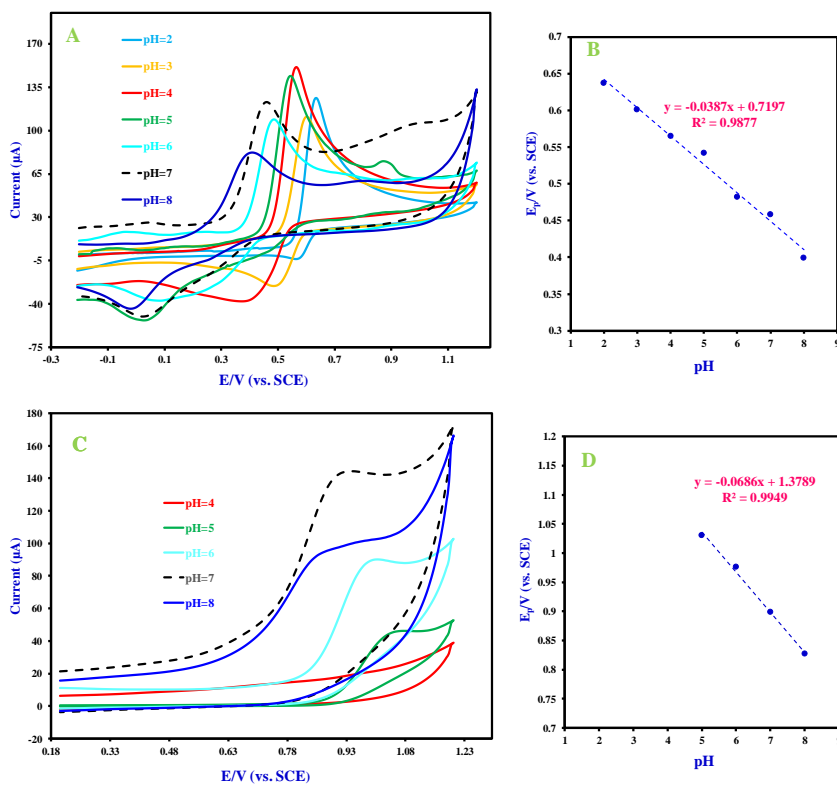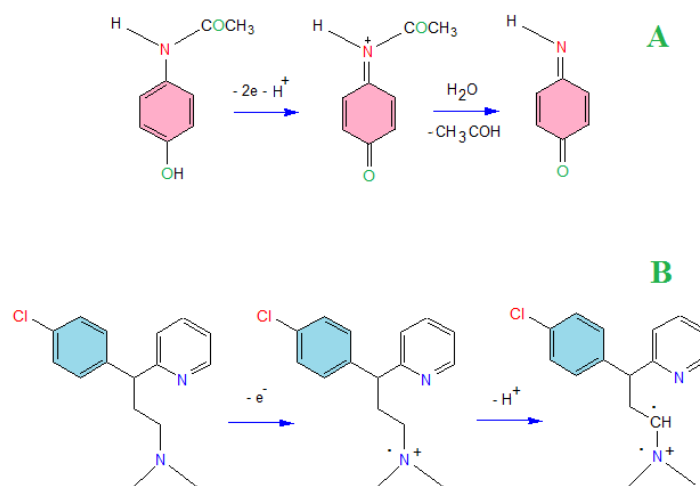

Figure 5. Effect of pH on the electro-oxidation of 1mM of AC (A and B) and CP (C and D) at surface of CPE/Fe$_3$O$_4$@SiO$_2$-NH$_2$/CoSB, (B, D): Plot of the oxidation peaks potential vs. the pH solution.

Scheme 2. Proposed mechanism for oxidation of AC (A) and CP (B).

that with the increase in pH, the anodic peak potentials (E_{pa}) for both species, shifted towards more negative values, which illustrates the involvement of hydrogen ions in the electro-oxidation of AC and CP. The suggested mechanisms of the electrochemical reactions of AC and CP on the CPE/Fe$_3$O$_4$@SiO$_2$-NH$_2$/CoSB are shown in Scheme 2A-B. As can be seen from Figure 5A, for AC maximum anodic peak current is at pH 4, and more than it decrease. Meanwhile, for CP, no anodic peak current was observed at very low pH (≤4) and it increased with increasing the electrolyte pH until 7.0. So, pH7.0 (PB, 0.1 M) was selected as an appropriate supporting electrolyte for the simultaneous determination of AC and CP.

Distinguishing voltammetric peaks of binary mixture (AC-CP) at the surface of CPE/Fe$_3$O$_4$@SiO$_2$-NH$_2$/CoSB

Figure 6 illustrates the cyclic voltammograms of the mixture of 1 mM AC and CP obtained under PB (0.1M, pH 7) at the surface of bare CPE (curve a) and CPE/Fe$_3$O$_4$@SiO$_2$-NH$_2$/CoSB (curve b). As shown in Figure 6, the electro-oxidation of AC

and CP at bare CPE surface show two poor oxidation peaks at 0.497 V and 0.934 V. Compared to the electrochemical response of the unmodified CPE, the peaks current signals of AC and CP acquired at the CPE/Fe$_3$O$_4$@SiO$_2$-NH$_2$/CoSB clearly enhanced and the corresponding oxidation peak potentials moved negatively (0.464 V and 0.910 V, respectively). In addition, a good peak separation between the electro-oxidation peaks of AC and CP was observed at surface of modified electrode. The enhancement on the anodic current and lowering of oxidation overpotential showed that the electron transfer kinetics for both compounds improves dramatically at the of CPE/Fe$_3$O$_4$-NH$_2$/CoSB sensor.

Moreover, the CV responses of the different interfering compounds such caffeine, diphenhydramine and phenylephrine in the mixture containing 1 mM AC and CP to evaluate the selectivity of the proposed nanosensor were individually examined. In this study, the presence of these compounds do not interfere with the detection of AC but diphenhydramine and phenylephrine affect the CP response because they have the same oxidation potentials with CP.

Figure 6. CV curves in the mixture of 1mM AC and CP in PB (0.1M, pH 7) at the surface of bare CPE (curve a) and CPE/Fe₃O₄@SiO₂-NH₂/CoSB (curve b) at scan rate 100 mV s⁻¹.
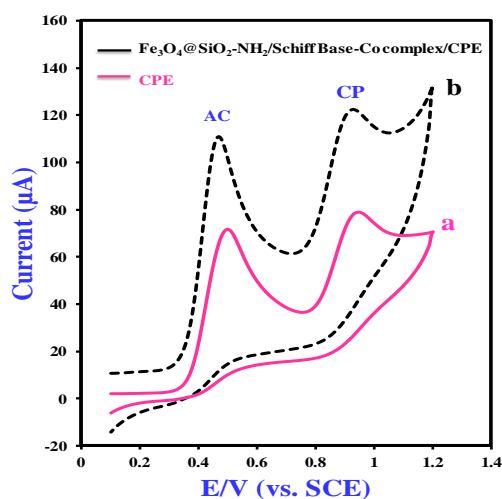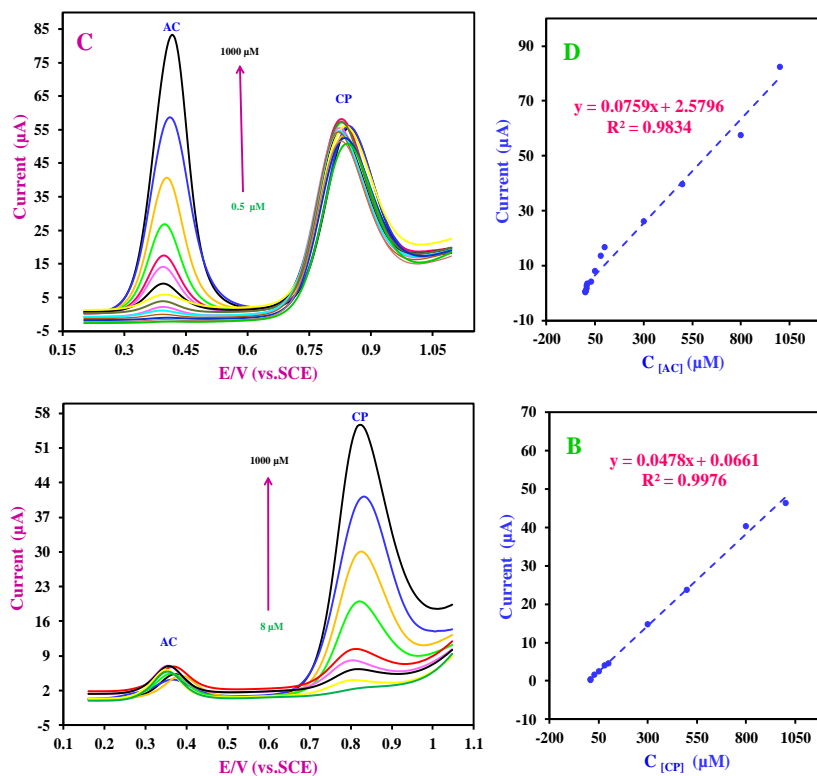

Figure 7. DPV profiles measured at the surface of CPE/Fe₃O₄@SiO₂-NH₂/CoSB in binary mixture of AC and CP in PB (0.1M, 7.0).

Analytical Measurements

Differential pulse voltammetry (DPV) method was applied for quantification of AC and CP as a sensitive techniques [29]. In binary mixture of AC and CP, the oxidation processes were investigated by varying the concentration of one of the two species whereas the concentrations of the other species kept constant. Figure 7A illustrates the DPV graphs of various

concentration of AC in the presence of a constant background of 1.0×10^{-3} M of CP, in 0.1 M PB at pH 7.0. It can be observed from Figure 7(A-B) that the peak current linearly increased with increasing the concentration of AC from 5×10^{-7} M to 1×10^{-3} M in the presence of a constant concentration of CP, while the response of chlorpheniramine remained unaltered. The linear equation was I_{pa} (µA) = 0.0759 C (µM) +

2.579, with a correlation coefficient of R^2 = 0.9834. Similarly, Figure 7C displays DPV curves of various concentrations of CP containing 5×10^{-5} M AC. A good linear relationship between the peak signals versus concentration of CP was exhibited in the range of 8×10^{-6} M to 1×10^{-3} M. The linear equation for chlorpheniramine was I_{pa} (μA) = 0.0478 C (μM) + 0.0661, with a correlation coefficient of R^2 = 0.9976. Detection limit (LOD) for AC and CP were estimated as 4.92×10^{-7} M and 5.68×10^{-6} M (S/N=3), respectively.

To verify the applicability of the CPE/Fe$_3$O$_4$@SiO$_2$-NH$_2$/CoSB nanosensor, the recovery experiments for determination AC and CP in human serum sample and commercial tablets were done. For this purpose, the samples were prepared as in experimental Section and analyzed using the standard-addition technique. By comparing the slopes of the calibration curve and standard addition, recovery values were obtained for AC and CP. The obtained results are given in Table 1. Obviously, these results demonstrate the reliability and effectiveness of the proposed method for pharmaceutical dosages and real-sample analysis.

Table 1. Recoveries for spiked AC and CP in real samples

Sample	Recovery AC	Recovery PC
Human serum	102.50	94.04
AC tablet	95.17	-
PC tablet	-	96.26

Table 2. Comparison between some recent reports in electrochemical determination of AC and CP

Electrode	Modifier	LR (μM)		LOD (μM)		Real sample	Ref
		AC	CP	AC	CP		
GCE	ZIF-67/MWCNT-COOH/Nafion	0.1-20 20-100	-	0.07	-	Tablets	[30]
GCE	Co$_3$O$_4$/FeCo$_2$O$_4$	0.1-220	-	0.0288	-	Serum	[31]
GCE	MWCNT/ß-cyclodextrin	0.05-1 1-300	-	0.0115	-	Urine Tablet	[32]
CPE	Ethynylferrocene–NiO/MWCNT	0.8-600	-	0.5	-	Tablet	[33]
CPE	NiO/CNTs/DPID	0.8-550	-	0.3	-	Urine Tablet	[34]
GCE	Au/Pd/ reduced graphene oxide	1.0-250	-	0.3	-	Tablet	[35]
CPE	8,9-Dihydroxy-7-methyl-12H-benzothiazolo [2,3-b]quinazolin-12-one	5.0–500	-	1.0	-	Tablet	[36]
GCE	RGO-gold dendrite	0.07-3000	-	0.005	-	Urine Tablet	[37]
PGE	ds-DNA-PPyox/RGO	-	0.05-200	-	0.023	Urine Tablet	[7]
GCE	Polytyramine doped tris(2,2′-bipyridyl)Ru(II) complex	-	2–45	-	0.338	Tablet Syrup	[38]
GCE	MWCNTs	-	5-500	-	1.63	Serum	[39]
CPE	Nickel Phosphate Nanoparticles	750-700	50-10000	240	16	Tablet	[40]
CPE	**CPE/Fe$_3$O$_4$@SiO$_2$-NH$_2$/CoSB**	**0.5-1000**	**8-1000**	**0.492**	**5.68**	**Serum Tablet**	**This work**

The repeatability of the designed nanosensor was appraised by gathering responses from 10 successive measurements on the same electrode towards the electro-oxidations of 1 mM AC and CP. The experimental results indicated an excellent repeatability with a relative standard deviation (RSD %) of 3.0% and 3.3% for AC and CP, respectively. Moreover, reproducibility of the proposed electrode was checked. The RSD% values were found less than 5% which confirm good reproducibility of the suggested nanosensor. Table 2. Compares the analytical parameters for some recent reports. It shows our proposed sensor shows good analytical results.

Conclusion

In this research study, we developed a cobalt Schiff base complex supported on magnetite modified with silica (Fe_3O_4@SiO_2-NH_2/CoSB) as a reliable and sensitive electrochemical nanosensor for the simultaneous determination of acetaminophen (AC) and chlorpheniramine (CP). The developed nanosensor showed highly electrocatalytic activity for the oxidation of both drugs with negative changes in anodic peak potentials. In addition, an excellent separation between the voltammetric signals for these analytes achieved at the modified electrode, suggesting that the CPE/Fe_3O_4@SiO_2-NH_2/CoSB is an efficient and highly sensitive tool for the simultaneous determination of AC and CP. The proposed nanosensor exhibited wide linear range of 5.0×10^{-7} to 1.0×10^{-3} M for AC and 8.0×10^{-6} to 1.0×10^{-3} M for CP with detection limit of 4.0×10^{-7} M and 5.0×10^{-6} M, respectively. Furthermore, the CPE/Fe_3O_4@SiO_2-NH_2/CoSB modified CPE was efficiently employed for the analysis AC and CP in real samples (human urine and commercial tablets) and obtained satisfactory results. In conclusion, the proposed nanosensor can be a promising sensor for pharmaceutical applications and clinical research.

Disclosure statement

No potential conflict of interest was reported by the authors.

ORCID

Mandana Amiri [iD]**:** 0000-0001-8789-5692

References

[1] X. Zhang, K.P. Wang, L.N. Zhang, Y.C. Zhang, L. Shen, *Anal. Chim. Acta,* **2018**, *1036*, 26–32.

[2] M. Singh, A. Sahu, P.K. Singh, F. Verma, A. Rai, V.K. Rai, *Electroanalysis*, **2020,** *32*, 1516–1523.

[3] F. Li, R. Li, Y. Feng, T. Gong, M. Zhang, L. Wang, T. Meng, H. Jia, H. Wang, Y. Zhang, *Mater. Sci. Eng. C*, **2019**, *95*, 78–85.

[4] H. Beitollahi, A. Mohadesi, S. Mohammadi, A. Pahlavan, H. Karimi-Maleh, A. Akbari, *J. Mol. Liq.*, **2012**, *169*, 130–135.

[5] X. Chen, J. Zhu, Q. Xi, W. Yang, *Sens. Actuators B Chem.*, **2012,** *161*, 648–654.

[6] N. Shetti, D. Nayak, *Can. J. Chem.*, **2017**, *95*, 553–559.

[7] K. Moulaee, M.R. Ganjali, P. Norouzi, H. Beitollahi, *DARU J. Pharm. Sci.*, **2019**, 1–8.

[8] H.K. Sarılmışer, N.O. Özçelik, B.Ö. Arslan, M. Gökalp, A. Ustaoğlu, U.K. Dude, Z. Knezevic, *J. Chem. Metrol*, **2017**, *11*, 61–67.

[9] O. Pirol, M. Sukuroglu, T. Ozden, *E-J. Chem.*, **2011**, *8*, 1275–1279.

[10] B. Daravath, G. S. Reddy, S. Kamarapu, *Asian J. Pharm. Clin. Res.,* **2014**, *7*, 98–102.

[11] S.E. Vignaduzzo, T.S. Kaufman, *J. Liq. Chromatogr. Relat. Technol.* **2013**, *36*, 2829–2843.

[12] A. Ali, M. Ahmed, T. Mahmud, M. Qadir, K. Nadeem, A. Saleem, *Indian J. Pharm. Sci.*, **2015**, *77*, 515–521.

[13] R.S. Joshi, N.S. Pawar, R.L. Sawant, *Lat. Am. J. Pharm.,* **2010**, *29*, 1226–1230.

[14] R. Sawant, R. Joshi, P.L.L. Bhangale, *Asian J. Pharm. Res. Health Care*, **2011**, *3*, 23–28.

[15] H. G. Lou, H. Yuan, Z.R. Ruan, B. Jiang, *J. Chromatogr. B*, **2010**, *878*, 682–688.

[16] C. Celma, J. Allue, J. Prunonosa, C. Peraire, R. Obach, *J. Chromatogr. A*, **2000,** *870*, 77–86.

[17] H. Imanzadeh, N.K. Bakirhan, B. Habibi, S.A. Ozkan, *J. Pharm. Biomed. Anal.*, **2020**, *181*, 113096.

[18] H. Imanzadeh, N.K. Bakirhan, B. Habibi, S.A. Ozkan, *J. Electrochem. Soc***., 2019**, *166*, B1209–B1216.

[19] H. Imanzadeh, N.K. Bakirhan, B. Habibi, S.A. Ozkan, *J. Electrochem. Soc.*, **2019**, *166*, B933–B941.

[20] F. Ahmadi, T. Mahmoudi-Yamchi, H. Azizian, *J. Chromatogr. B,* **2018**, *1077*, 52–59.

[21] M. Amiri, A. Bezaatpour, Z. Pakdel, K. Nekoueian, *J. Solid State Electrochem.*, **2012**, *16*, 2187–2195.

[22] M. Amiri, Z. Pakdel, A. Bezaatpour, S. Shahrokhian, *Bioelectrochemistry*, **2011**, *81*, 81–85.

[23] S. Shahrokhian, M. Amiri, *J. Solid State Electrochem.*, **2007**, *11*, 1133–1138.

[24] S. Laurent, D. Forge, M. Port, A. Roch, C. Robic, L. Vander Elst, R.N. Muller, *Chem. Rev.*, **2008**, *108*, 2064–2110.

[25] H. Bagheri, A. Afkhami, M. Saber-Tehrani, H. Khoshsafar, Talanta, **2012**, *97*, 87–95.

[26] M. Esmaeilpour, A.R. Sardarian, J. Javidi, *Appl. Catal. A Gen.*, **2012**, *445*, 359–367.

[27] M. Mikani, R. Rahmanian, M. Karimnia, A. Sadeghi, *J. Chin. Chem. Soc.,* **2017**, *64*, 1446–1459.

[28] A. Bezaatpour, S. Khatami, K. Nejati, *J. Iran. Chem. Soc.*, **2017**, *14*, 2105–2115.

[29] L. Zhang, S. Li, J. Xin, H. Ma, H. Pang, L. Tan, X. Wang, *Microchim. Acta,* **2019,** *186*, 9.

[30] H. Guo, T. Fan, W. Yao, W. Yang, N. Wu, H. Liu, M. Wang, W. Yang, *Microchem. J.*, **2020**, *158**, 105262.

[31] Z. Lu, J. Zhong, Y. Zhang, M. Sun, P. Zou, H. Du, X. Wang, H. Rao, Y. Wang, *J. Alloys Compd.*, **2020**, *858*, 157701.

[32] A.U. Alam, Y. Qin, M.M. Howlader, N.X. Hu, M.J. Deen, *Sens. Actuators B Chem.*, **2018**, *254* 896–909.

[33] M.R. Shahmiri, A. Bahari, H. Karimi-Maleh, R. Hosseinzadeh, N. Mirnia, *Sens. Actuators B Chem.*, **2013**, *177*, 70–77.

[34] H. Karimi-Maleh, M.R. Ganjali, P. Norouzi, A. Bananezhad, *Mater. Sci. Eng. C*, **2017**, *73*, 472–477.

[35] H. Wang, S. Zhang, S. Li, J. Qu, *Talanta*, **2018**, *178*, 188–194.

[36] H. Karimi-Maleh, M. Moazampour, H. Ahmar, H. Beitollahi, A.A. Ensafi, *Measurement***, 2014**, *51*, 91–99.

[37] S. Yu, H. Li, G. Li, L. Niu, W. Liu, X. Di, *Talanta,* **2018**, *184*, 244–250.

[38] E.A. Khudaish, M. Al-Hinaai, S. Al-Harthy, K. Laxman, *Electrochim. Acta*, **2014**, *135*, 319–326.

[39] Z. Pourghobadi, R. Pourghobadi, *Int. J. Electrochem. Sci.*, **2015**, *10*, 7241–7250.

[40] A. Samadi-Maybodi, S.K.H. Nejad-Darzi, H. Ilkhani, *Anal. Bioanal. Electrochem.*, **2011**, *3*, 134–145.